Guided vortex motion in $YBa_2Cu_3O_7$ thin films with collective ratchet pinning potentials

A. Palau, C. Monton, V. Rouco, X. Obradors, and T. Puig
Institut de Ciència de Materials de Barcelona, ICMAB-CSIC, Campus de la UAB, E-08193 Bellaterra, Spain
(Received 21 November 2011; published 13 January 2012)

We investigate guided vortex motion in high-temperature $YBa_2Cu_3O_7$ thin films patterned with an array of asymmetric blind antidots. A preferential vortex motion along spatial asymmetric pinning potentials has been directly observed by changing the driving current direction. Transport measurements reveal that effective ratchet potentials are created by fixed vortices strongly pinned within the antidots while the spatial asymmetry is transferred to interstitial vortices. We study a novel ratchet system that requires vortex-vortex interactions to work, in contrast with the individual vortex effects studied in conventional ratchet systems. By tuning the magnetic field and temperature, we are able to control the transition from a single vortex pinning regime to a region where collective effects become important and determine the range where the rectification effect is activated.

DOI: 10.1103/PhysRevB.85.012502 PACS number(s): 74.25.Wx, 74.25.Sv, 74.72.−h

The individual and collective behavior of vortices in type-II superconductors is of enormous practical significance for applications. This has sustained the study of vortex dynamics and methods for understanding the fundamental properties of vortex motion in superconductors with artificial pinning centers. In particular, a new generation of solid-state devices can be achieved by exploiting the manipulation of flux quanta, such as flux pumps, vortex diodes, and lenses to concentrate magnetic flux.[1] Thus, many experiments involving patterned thin films with arrays of dots or antidots have been developed in order to control the strength and location of the pinning centers.[2–4] With regard to directed transport at the nanoscale, advances in nanofabrication have enabled investigations of guided vortex motion, whose direction can be determined by asymmetric pinning potentials. The mechanism responsible for this phenomenon is called the ratchet effect, and it can also be found in biological systems, such us bimolecular motors and molecular machines, or in Brownian motors.[5–7] The study of ratchets in superconductors can be used to analyze and understand the mechanisms involved in this phenomenon, tailored by the external parameters, namely temperature (T) and magnetic field (H).

Most studies of ratchets focus on vortex motion at fields below the matching field, where a single vortex moves on a nonsymmetrical pinning potential, the so-called one-particle ratchet. In this kind of ratchet, for magnetic fields above the first matching field, interplay between interstitial and pinned vortices was observed in some low-temperature superconductor (LTS) systems, producing sign reversals by tuning the density of the vortex lattice.[8–10] However, recently a new type of ratchet system was theoretically proposed and modeled[11] in which individual vortex pins are not at the origin of the ratchet pinning potential. Instead, the asymmetric pinning potential is created by vortices trapped in nonsymmetric artificial pinning sites that transfer the asymmetry to weakly pinned interstitial vortices through their interaction. This kind of ratchet, which appears as a consequence of the long-range interaction between vortices, has been called a "collective interaction-driven ratchet." In this work, we experimentally demonstrate this new type of vortex ratchet, which requires collective interactions to work.

Asymmetric pinning potentials can be created with many different techniques.[12] Toward that end, numerous studies have been performed using LTS's, where the intrinsic vortex pinning is low enough to easily introduce effective artificial pinning centers. For this purpose, one of the most effective systems consists of patterning nonsymmetric magnetic nanodots in superconducting films.[10,13] Moreover, nonsymmetric potentials have been obtained from arrays of asymmetric antidots due to vortex/hole interactions.[9,14] Other approaches have considered the generation of local symmetries by introducing low pinning channels of easy vortex motion.[15,16] In all these systems, maximum guided vortex motion was observed at low H (close to their matching fields of several Oe) and at T near T_c in order to avoid enhanced intrinsic pinning. Controlled vortex motion in high-temperature superconducting (HTS) thin films appears to be much more complicated due to the strong influence of thermal fluctuations and high intrinsic pinning. Rectification resistance due to vortex unpinning was observed in Bi2212 single-crystal films with a low amount of disorder. In this case, matching and ratchet effects were found at high T and very low H.[17] Guided vortex motion at low currents, $I < I_c$, was measured in YBCO thin films with asymmetric arrangements of symmetric antidots via resistive Hall-type experiments.[18] In contrast to vortex motion due to unpinning at $I > I_c$, they could analyze transverse rectification at low T. Thus, although some rectifying effects have been observed in HTS systems, the nature of the pinning interaction at high fields, where collective effects start to dominate, has yet to be explored.

In this contribution, we aim to study guided vortex motion mechanisms in high-J_c YBCO thin films with a strong contribution of intrinsic pinning centers. We are exploring vortex rectification effects in HTS, controlled by collective interaction between interstitial vortices and a vortex strongly pinned in asymmetric antidots. By tuning H and T, the vortex array undertakes single vortex pinning to a vortex-vortex interaction transition, which determines the region where the rectification effect is activated. The mechanism proposed to explain the collective ratchet effect observed in this system is similar to the one modeled in Ref. 11 in that it requires collective interactions to work, thus no ratchet signal is expected when there are no interstitial vortices. This is what we observe in our nanostructured HTS thin films, although

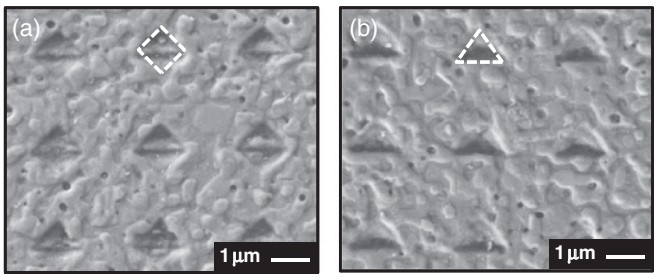

FIG. 1. SEM pictures of a YBCO bridge patterned with diamond (a) and triangular (b) blind antidots.

in our case we are able to observe the ratchet effect at low temperatures and at fields well above the matching field (hundreds of mT). We explore different artificial lattices with ordered arrays of symmetric and asymmetric blind antidots (which do not perforate the superconductor completely). The latter give rise to an asymmetric response in the critical currents that is associated with a preferential direction of vortex motion.

Epitaxial YBCO films that are 250 nm thick were grown on $LaAlO_3$ single-crystal substrates using a metalorganic decomposition method based on a trifluoroacetate precursor route.[19] They were patterned by optical lithography to form 100×20 μm bridges with four electric contacts for transport measurements. We used high-quality films with $\Delta\omega < 1^o$, $\Delta\phi < 1^o$, a surface roughness of $\sim$25 nm, and self-field critical current density, J_c (77 K) $\sim$ 3.5 MA/cm^2. Artificially patterned lattices with blind antidots were performed on the bridges by focused ion beam (FIB) lithography using a Zeiss 1560XB Cross Beam. We studied a YBCO thin film with three identical transport bridges. One of the bridges was patterned with triangular blind antidots, another with diamonds, and the last one was used as a reference. In both cases, the blind antidots were 2.4 μm apart and had a depth of 80 nm. Figure 1 shows scanning electron microscopy (SEM) images of the arrays of symmetric and asymmetric blind antidots patterned in the YBCO films. A standard four-terminal transport technique was used to perform the transport measurements in a Quantum Design PPMS in a range of H from 0 to 9 T and T from 50 to 77 K. In-field transport measurements were carried out in a maximum Lorentz force configuration with H perpendicular to the film plane. The pinning force was calculated with the critical current value determined using a 20 μV/cm criterion.

In Fig. 2, we show the pinning force versus magnetic field $F_p(H)$, measured at 77 K, for the reference bridge and the bridges with arrays of antidots. It is worth noting at the outset that the curves $F_p(H)$ obtained for the bridges with the blind antidots are higher than that of the reference bridge, showing an increase of the maximum F_p from 2.3 to 3.3 GN/m^3. This result shows that with the FIB patterning, we create artificial defects that act as strong pinning sites (stronger than intrinsic natural defects). Thus, vortex motion in the systems with blind antidots will be controlled by the artificial pinning potentials. Furthermore, we observed that both types of defects (triangles and diamonds) induce similar $F_p(H)$ curves, indicating that they are equally effective vortex pinning sites. No significant changes are observed in the critical current density at low fields, as is shown in the inset of Fig. 2. However, we will see below that relevant effects are observed when we invert the sign

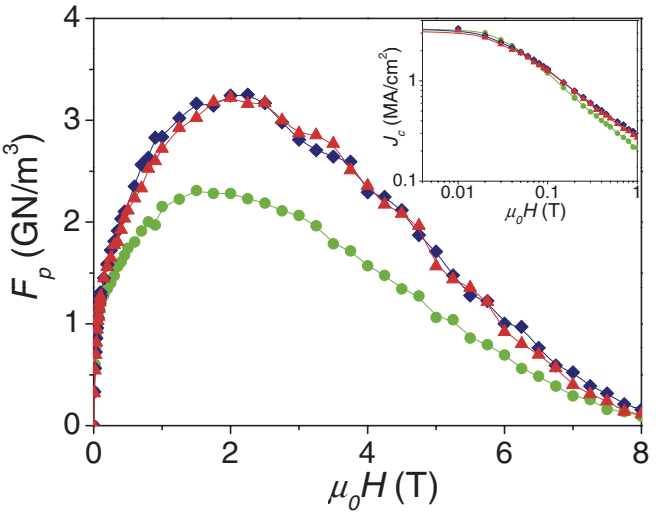

FIG. 2. (Color online) $F_p(H)$ obtained at 77 K for a reference bridge (dots) and for bridges with triangular (triangles) and diamond (diamonds) blind antidots. The inset shows the corresponding $J_c(H)$ dependence at low fields.

of the current direction. In order to estimate the relevance in the pinning effect of the implanted Ga^+ generated by FIB, the penetration depth of the Ga+ ions in the YBCO sample and the distribution of the density of vacancies as a function of sample depth were estimated using Monte Carlo simulations.[20] For this purpose, we have taken into account the sample's density, the energy of the Ga+ ions (30 KV), and the ion current used (100 pA). This estimation shows that all the processes related to the Ga^+ interaction (implantation, amorphization, and vacancy generation) lie within a 10-nm-thick superficial layer in the irradiated region. Since the bottom YBCO layer in blind antidots is 170 nm thick, we consider that the FIB damaged region is not relevant to the overall pinning effect. We assume then that the mechanism leading to vortex pinning in our systems can be assigned to the local spatial thickness modulation, which produces a reduction of the vortex line free energy given by[21]

$$E_l = \varepsilon_0 t \ln \frac{\lambda}{\xi}, \quad (1)$$

where we have taken the vortex length, t, equal to the YBCO layer thickness, ε_0 is the vortex self-energy, $\varepsilon_0 = (\phi_0/4\pi\lambda)^2$, λ is the penetration depth, and ξ is the coherence length. Considering the thickness of the YBCO layer (250 nm) and the thickness of the bottom layer inside the blind antidots (170 nm), a reduction of 32% in E_l is obtained when vortices are nucleated inside the artificial defects. Consistent with this, we observe an enhancement of the maximum pinning force of $\sim$30% in the bridges with blind antidots (see Fig. 1) that will tend to confine the vortices strongly pinned within the artificial defects. Confinement effects have also been observed in LTS films with large blind antidots, attributed to the normal/superconductor boundary condition that flux lines encounter at mesoscopic blind holes.[22,23]

The effect of blind antidot geometry in the vortex dynamics has been analyzed by measuring the current-density–electric-field curves (J-E) under positive, J^+, and negative, J^-, applied

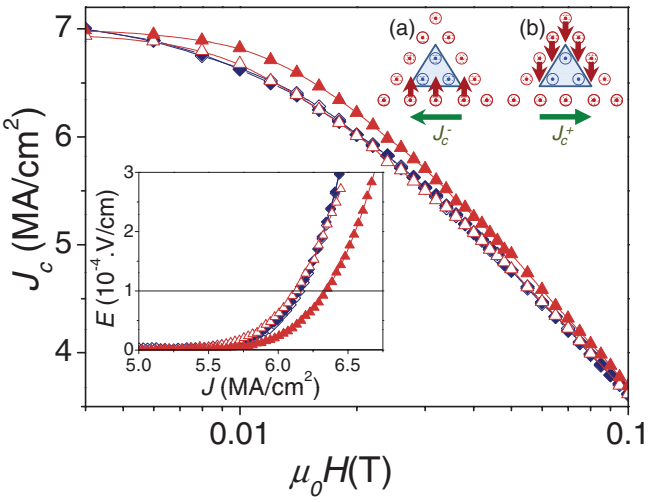

FIG. 3. (Color online) $J_c(H)$ measured at 65 K for a bridge with triangular (triangles) and diamond (diamonds) blind antidots, by applying positive, J_c^+ (open symbols), and negative, J_c^- (closed symbols), current. The lower inset shows the positive and negative branches of J-E curves found for the same bridges at 65 K and 20 mT. The line shows the electric field criteria chosen to determine J_c. The higher inset shows a schematic drawing of interstitial vortex motion under negative (a) and positive (b) current. The vortex pinned inside the antidots is shown in blue and the interstitials in red.

dc current. By inverting the sign of the current, we are inverting the sign of the Lorentz force ($\boldsymbol{F_L} = \boldsymbol{J} \times \boldsymbol{B}$) and thus measuring the pinning response along symmetric and asymmetric pinning potentials. Results are plotted in the inset to Fig. 3, where we compare the negative, J^-, and positive, J^+, branches of the J-E curves at 20 mT and 65 K. For a direct comparison, we show both J^+ and J^- in the same quadrant. We observe that in the bridge with triangular pinning sites, there is a marked dependence on the F_L direction. This effect appears as an asymmetric response in the J-E curve. However, the curves obtained for the bridge with diamonds are independent of the F_L direction, showing a symmetric J-E response. By performing the same measurements at different H, we have determined the field dependence of the critical current density under positive external current, $J_c^+(H)$, and negative external current, $J_c^-(H)$. Figure 3 shows the curves obtained at 65 K for the bridges with symmetric and asymmetric pinning potentials. We have used a criterion of 100 μV/cm to determine J_c in order to better observe the differences in $J_c(H)$. Note that the bridge with a triangular blind antidot exhibits a clear difference between $J_c^-(H)$ and $J_c^+(H)$, with a maximum of the order of 0.15 MA/cm^2 at 20 mT. In contrast, for the bridge with diamonds, no difference in the $J_c(H)$ curves is observed when F_L is reversed. On the whole, the results show that the asymmetric pinning potentials produce a preferential direction of vortex motion that is effective up to high magnetic fields ($\sim$0.1 T at 65 K) and is clearly detected as an asymmetric response of J_c.

In order to understand the dissipation mechanisms involved in the ratchet effect of our systems, we have to consider two different populations of vortices. Vortices inside the blind antidots, v_{ant}, strongly pinned with a force, $F_p{}^{\text{ant}}$, and interstitial vortices, v_{inter}, which are located outside them with a weaker pinning force, $F_p{}^{\text{inter}} < F_p{}^{\text{ant}}$. It is important to note that the matching field associated with the array of blind antidots studied should be 0.4 mT, much lower than the field step used in the measurements (2 mT). Thus, we start with a system with a large number of interstitial vortices that will start to move for currents lower than the depinning current of vortices within the antidots and will feel the spatial asymmetry through their interaction. Considering the sample geometry, the triangular antidot fractional area that will determine the ratio between pinned/interstitial vortices is 1/12.

Further evidence that asymmetric dissipation occurs from interstitial movement comes from the fact that the curve $J_c^-(H)$ measured for the bridge with triangles goes above the other ones. In this configuration, interstitial vortices must flow against a row of fixed vortex at the base of the triangles [scheme (a) in Fig. 3], which require a larger F_L than that necessary to overcome vortices pinned at the tilted edges of the triangles [scheme (b) in Fig. 3]. In the last case, interstitial vortices have a very similar pinning potential to that created by the vortices fixed in the diamonds, and hence very similar $J_c(H)$ curves are found. We conclude, therefore, that in the range of H where we observe a difference between J_c^+ and J_c^-, the critical current density is determined by the motion of interstitial vortices. Dissipation due to interstitial vortex motion was observed in LTS film with triangular magnetic dots[10] when interstitial vortices exceeded the number of vortices trapped inside the dots. In that case, the experiment was performed up to several matching fields.

In the following, we will evaluate the range of H and T where the ratchet effect is relevant. Figure 4(a) shows the field dependence of $[J_c^+$-$J_c^-]$ obtained at 65 K for the three bridges analyzed. As observed in the $J_c(H)$ curves shown in Fig. 3, the asymmetric response of J_c with the current direction is only relevant for the bridge with asymmetric pinning potential (triangles). As discussed above, the asymmetric potential is created due to the interaction of interstitial vortices with those fixed in the triangular antidots. Thus, for the collective ratchet to be observable, (i) the pinning force within the antidots must be higher than that outside ($F_p{}^{\text{inter}} < F_p{}^{\text{ant}}$) so that there will be vortices trapped in the asymmetric pinning centers for a given F_L able to move interstitials, (ii) the interaction between vortices inside the antidots and interstitials (v_{ant}-v_{inter}) must be strong enough that v_{inter} motion feels the asymmetric pinning potential, and (iii) the number of fixed vortices within the antidots must be low enough to preserve the asymmetry imposed by the edge of the triangles. At very low fields, requirement (ii) is not satisfied and thus $[J_c^+$-$J_c^-] \sim 0$. At large fields ($\mu_0 H > 0.1$ T at 65 K), (v_{ant}-v_{inter}) interactions must be strong enough to overtake the difference between $F_p{}^{\text{inter}}$ and $F_p{}^{\text{ant}}$, causing motion of both populations of vortices. Requirement (iii) depends on the fraction of vortices trapped at the edge of the triangular blind holes. This is quantified in the inset to Fig. 4(a), where we show the density of vortices located at the edge of the triangles and the density of those pinned inside them as a function of H. As a first approximation, we have assumed homogeneous distribution of vortices in the sample, although vortex density inside the blind antidots must be slightly higher than that outside due to their strong pinning potential. With this simple approximation, we observe that for $\mu_0 H > 0.1$ T, where the ratchet effect disappears, the

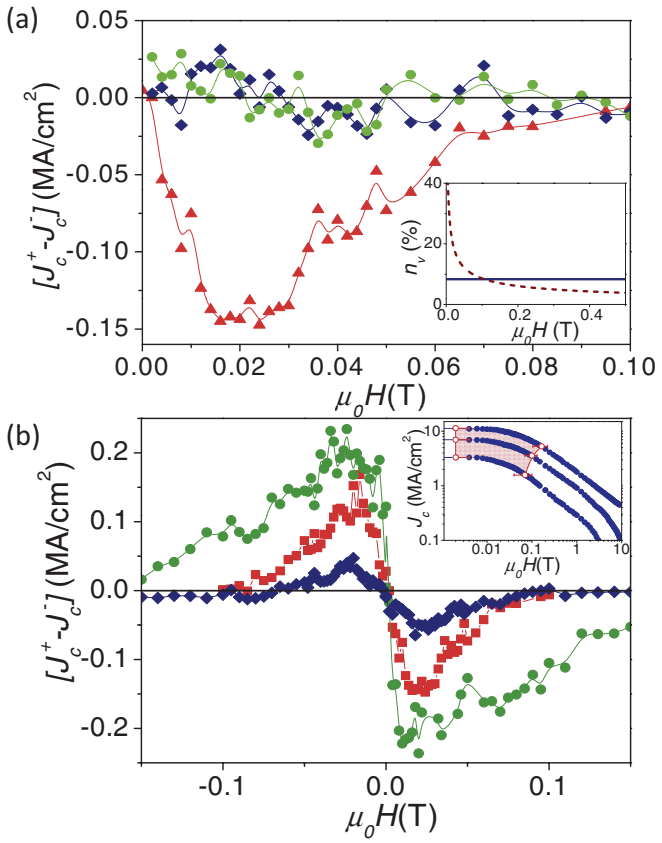

FIG. 4. (Color online) (a) Magnetic-field dependence of $[J_c^+ - J_c^-]$ obtained at 65 K for a reference bridge (dots), a bridge with triangular (triangles) and diamond (diamonds) blind antidots. The inset shows a quantitative estimation of vortex density located at the edge of the triangles (dashed line) and inside them (solid line) (b) Magnetic-field dependence of $[J_c^+ - J_c^-]$ found for a bridge with triangles at 77 K (diamonds), 65 K (squares), and 50 K (dots). The inset shows the $J_c(H)$ curves measured at 77, 65, and 50 K, where we have shadowed the region where the ratchet effect is occurring.

population of vortices located at the edge of the antidots, which feels the triangular asymmetry more strongly, starts to be lower than that of vortices located inside the blind antidots.

Overall, our results show that guided vortex motion occurs when vortices trapped inside the pinning sites interact with depinned interstitial vortices. At the minimum applied field used in the experiment, the mean distance between vortices is about 1 μm and thus there are already more than two vortices inside the artificial pinning centers. According to this description, the ratchet effect is effective in a range of fields in which interactions between v_{ant} and v_{inter} are of the same order as the interaction of v_{ant} with blind antidots, i.e., the region between individual and collective vortex motion regimes. As has already been established for YBCO thin films,[24,25] a log-log $J_c(H)$ curve sets the scale for the transition from a low-field J_c plateau, associated with single-vortex pinning, to a power-law region dominated by collective effects. The crossover between these two regimes is associated with different temperature-dependent interactions between the vortex lattice and the pinning defects. In Fig. 4(b), we show the asymmetric behavior of $J_c(H)$ at different T. One of the most remarkable features observed is that the ratchet effect is extended to higher fields for lower temperatures. Accordingly, the sign of $[J_c^+ - J_c^-]$ is reversed by inverting the direction of the applied field, since we are inverting the F_L direction. By analyzing the $J_c(H)$ behavior at different T for the bridge with triangular blind holes [inset to Fig. 4(b)], it is possible to establish a correlation between the range of fields where the ratchet effect is relevant and the crossover from single to collective vortex pinning regimes (shadowed region in the plot). Hence, we have generated a system with very efficient asymmetric pinning sites where guided vortex motion can be controlled in a wide range of fields, and temperature can be tuned.

In conclusion, we have patterned lattices of symmetric and asymmetric blind antidots by FIB in YBCO bridges. Transport experiments show that those artificial pinning potentials enhance the pinning force created by intrinsic defects. We have also found that when positive and negative external currents are applied in the bridge with asymmetric blind holes, a preferential direction of vortex motion (the ratchet effect) appears in a certain range of applied magnetic fields, depending on temperature. We propose that the ratchet effect is generated by the motion of interstitial vortices that interact with the fixed vortices strongly pinned within the blind antidots. This effect disappears when the v_{ant}-v_{inter} interaction becomes strong enough to force the motion of vortices pinned inside the blind antidots. A clear correlation has been observed between the range where the ratchet is effective and the region where vortex-vortex interaction competes with vortex-defect interaction.

The authors are grateful to J. Llobet, X. Borrisé, and the GICSERV project for FIB technical support. We acknowledge the financial support from MICINN (MAT2008-01022, Consolider NANOSELECT), CSIC (PIE-200860I209), and EU (HIPERCHEM and NESPA). V.R. would like to thank CSIC for financial support.

[1] S. Savel'ev and F. Nori, Nat. Mater. **1**, 179 (2002).
[2] K. Harada *et al.*, Science **274**, 1167 (1996).
[3] J. I. Martin *et al.*, Phys. Rev. Lett. **79**, 1929 (1997).
[4] M. Velez *et al.*, J. Magn. Magn. Mater. **320**, 2547 (2008).
[5] R. D. Astumian and P. Hanggi, Phys. Today **55**(11), 33 (2002).
[6] J. Howard, Nature (London) **389**, 561 (1997).
[7] J. Prost *et al.*, Phys. Rev. Lett. **72**, 2652 (1994).
[8] L. Dinis *et al.*, Phys. Rev. B **76**, 212507 (2007).
[9] C. C. D. Silva *et al.*, Nature (London) **440**, 651 (2006).
[10] J. E. Villegas *et al.*, Science **302**, 1188 (2003).
[11] C. J. Olson *et al.*, Phys. Rev. Lett. **87**, 177002 (2001).
[12] B. L. T. Plourde, IEEE Trans. Appl. Supercond. **19**, 3698 (2009).

[13] A. V. Silhanek *et al.*, Appl. Phys. Lett. **90**, 182501 (2007).
[14] B. Y. Zhu *et al.*, Phys. Rev. B **68**, 014514 (2003).
[15] Y. Togawa *et al.*, Phys. Rev. Lett. **95**, 087002 (2005).
[16] K. Yu *et al.*, Phys. Rev. B **76**, 220507 (2007).
[17] S. Ooi *et al.*, Physica C **468**, 1291 (2008).
[18] R. Wordenweber *et al.*, Phys. Rev. B **69**, 184504 (2004).
[19] T. Puig *et al.*, Supercond. Sci. Technol. **18**, 1141 (2005).
[20] J. F. Ziegler *et al.*, *The Stopping and Ranges of Ions in Matter* (Pergamon, New York, 1985), vol. 1.
[21] G. Blatter *et al.*, Rev. Mod. Phys. **66**, 1125 (1994).
[22] G. R. Berdiyorov *et al.*, New J. Phys. **11**, 013025 (2009).
[23] A. Bezryadin *et al.*, Phys. Rev. B **53**, 8553 (1996).
[24] B. Dam *et al.*, Nature (London) **399**, 439 (1999).
[25] A. Palau *et al.*, Phys. Rev. B **73**, 132508 (2006).